PERGAMON

Solid State Communications 112 (1999) 605–610

solid state communications

www.elsevier.com/locate/ssc

Inelastic electron scattering from a quasi-one-dimensional electron gas

M.S. Kushwaha[a,*], P. Zielinski[b]

[a]*Institute of Physics, University of Puebla, P.O. Box J-48, Puebla 72570, Mexico*
[b]*Institute of Nuclear Physics, Radzikowskiego 152, 31-342 Krakow, Poland*

Received 27 May 1999; received in revised form 15 July 1999; accepted 26 August 1999 by A. Pinczuk

Abstract

A theoretical investigation has been made of the fast-particle energy-loss to a quasi-one-dimensional electron gas (Q1DEG) within the framework of the random-phase-approximation (RPA). For this purpose, we use an exact expression for the inverse dielectric function and the parabolic potential to characterize well the lateral confinement. Three geometries are considered: the fast-particle moving parallel to, being specularly reflected from, and shooting through the Q1DEG. The illustrative numerical examples lead us to infer that the dominant contribution to the loss peaks comes from the intra- and intersubband collective excitations. We argue that high resolution electron energy loss spectroscopy (HREELS) could prove to be a potential alternative of the existing optical techniques.

Keywords: A. Nanostructures; A. Quantum wells; D. Dielectric responses; D. Electron–electron interactions; E. Electron energy loss spectroscopy

Progress in nanofabrication technology and the ability to tailor potentials and interactions is stimulated by the world-wide drive to develop exotic high-speed, low-power devices that are small enough, sharp enough, or uniform enough to behave the way theory says they should. These are quantum structures-nonoscale layers, channels, and boxes known as quantum wells, quantum wires, and quantum dots—in which the broad energy bands of conventional semiconductors squeeze into more sharply defined energy levels. Moreover, that is a transformation that promises greater speed and efficiency for the resulting optical and electronic devices.

Past research on quantum structures has focused on layered structures, quantum wells and superlattices, for example, that confine conduction electrons to two dimensions. Now, systems in which the electrons are confined to one dimension of free motion (quantum wires) are providing materials with remarkable new phenomena. An early motivation behind the proposal of quantum-wire structures was the suggestion [1,2] that one-dimensional *k*-space restrictions would severely reduce the impurity scattering, thereby substantially enhancing the low-temperature electron mobilities. As a result, the technological promise that emerges, are the routes to faster transistors and optoelectronic devices fabricated out of quantum wire structures.

Research interest burgeoned in quantum wires not only because of their potential device applications but also because of the fundamental physics involved. For instance, they have offered us an excellent opportunity to study the real one-dimensional Fermi gases in a relatively controlled manner. Such (isolated and multiple) quantum wires, with active widths (along the plane of confinement) less than 30 nm and of negligible (less than 10 nm) thickness, have already been fabricated [3,4] and continued advancements in the growth and fabrication techniques are expected to provide even sharper wires in the near future. Apart from the fact that the question of whether the one-dimensional (1D) electron system is better described as a Luttinger liquid or as a Fermi liquid is still open [5,6], all experimental results [7,8] hitherto seem to be explicable on the basis of a normal Fermi-liquid model [9,10].

The purpose of this letter is to report the first theoretical investigation on the fast-particle energy loss to a quasi-one-dimensional electron gas (Q1DEG). This has been carried

* Corresponding author.

0038-1098/99/$ - see front matter
PII: S0038-1098(99)00413-5

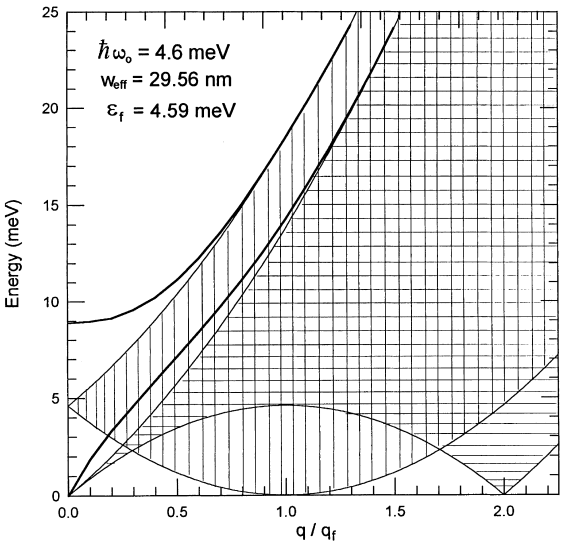

Fig. 1. Excitation spectrum of a Q1DEG within a two-subband model. The horizontally (vertically) hatched region refers to the intrasubband (intersubband) single-particle excitations associated with the lowest occupied (first excited) subband at absolute zero, where $\mathrm{Im}\Pi_{11}(\mathrm{Im}(\chi_{12} = \Pi_{12} + \Pi_{21}) \neq 0$. The bold lower (upper) curve represents the intrasubband (intersubband) collective excitations.

out in the framework of a dielectric response theory (DRT) [11–13], which is still the best available description of electron-energy-loss spectroscopy (EELS). The DRT has been successfully used to study the multisubband superlattice systems [14,15] and provided an excellent interpretation of the high resolution electron-energy-loss spectroscopy (HREES) experiments [16,17] on GaAs–AlGaAs superlattices for all the electron impact energies (from 4 to 35 eV). DRT proceeds in two steps. The first step consists in evaluating the work done by the polarization field of the sample on the electron (responsible for the polarization) along its semiclassical trajectory in which the electron is regarded as an external time-dependent potential that causes transitions in the target. This first, classical step is complemented by a suitable quantal description of the multiple excitations emitted or absorbed by the electron. The essential result of the second step is accomplished by confining ourselves within the random-phase approximation (RPA), so that the exchange–correlation effects are neglected.

In order to define the quantum wire, we start with an electron gas in a narrow quantum well with interfaces parallel to the $\hat{x} - \hat{y}$ plane and the well-width smaller than any other length scale in the problem. This corresponds to a realistic experimental situation in which only the lowest subband in the quantum well is occupied, so the motion of the electrons along the $\hat{z}$-direction is ignored. We consider an effective confining potential, (which is a sum of bare and Hartree potential) along the $\hat{y}$-direction to be parabolic one (which is quite a reasonable approximation for low density in GaAs quantum wires [18,19]). Thus, a fabricated quantum wire represents a Q1DEG with free electron motion along the $\hat{x}$-axis, and the subband structure along the $\hat{y}$-axis. For this parabolic confinement [$V(y) = m^*\omega_0^2 y^2/2$, with m^* as the electron effective mass and ω_0 as the frequency of harmonic potential], the single-particle eigenstates and eigenenergies are given by $\psi_{nk}(x,y,z) = L_x^{-1/2}\, \mathrm{e}^{\mathrm{i}kx}\phi_n(y)[\delta(z)]^{1/2}$ and $E_{nk} = (n + 1/2)\hbar\omega_0 + \hbar^2k^2/(2m^*)$, where n is the subband index and $\phi_n(y)$ is the Hermite function. L_x refers to the finite length (along the $\hat{x}$-axis) of the quantum wire and the transverse confinement length of the electron is $l_0 = [\hbar/m^*\omega_0]^{1/2}$. While the details of the analytical results are deferred to a long publication, we would like to specify the strategy of the present numerical work. We are interested in this paper to explore a simple situation of a two subband model with only the lowest one occupied. We do so by calculating self-consistently the Fermi energy (ε_f) for a given particle density ($N_\mathrm{e}^{1\mathrm{D}}$) and confining potential strength ($\hbar\omega_0$) through

$$N_\mathrm{e}^{1\mathrm{D}} = \frac{2}{\pi\hbar}\sum_n [2m^*(\varepsilon_\mathrm{f} - \varepsilon_n)]^{1/2}\theta(\varepsilon_\mathrm{f} - \varepsilon_n) \tag{1}$$

where $\varepsilon_n = (n + 1/2)\hbar\omega_0$. For $\hbar\omega_0 = 4.6$ meV and $N_\mathrm{e}^{1\mathrm{D}} = 5.72 \times 10^5 \mathrm{cm}^{-1}$, Eq. (2) yields $\varepsilon_\mathrm{f} = 4.59$ meV, which corresponds to the Fermi level lying just around the bottom of the first excited subband. The effective confinement width of the parabolic potential well, estimated by the extent of the Hermite function ($w_\mathrm{eff} = 2\sqrt{2n+1}\,l_0$), comes out to be 31.45 nm. The actual w_eff which we estimated from a fit to the hard wall potential is $w_\mathrm{eff} = 29.56$ nm. The difference indicates that the actual confinement potential is somewhere between square and parabolic [18,19].

The EELS refers, in a broad sense, to every kind of electron spectroscopy wherein inelastic electron scattering is used to study excitations of surfaces or thin solid films. We have studied the fast-particle energy loss phenomenon in three different geometries with respect to the motion of a coherent electron beam: the fast-particle moving parallel to, being specularly reflected from, and shooting through the Q1DEG. It should be pointed out that the inverse dielectric function $\varepsilon^{-1}(q,\omega;y,y')$ of the Q1DEG is central to the description of energy loss phenomena. The exact inverse dielectric functions (IDF) for quasi-n-dimensional (with $n = 2, 1, 0$) electron systems were derived in Ref. [20] for multiple subband occupancy within the RPA. The IDF for a Q1DEG is given by [20]

$$\varepsilon^{-1}(y,y') = \delta(y - y') + \sum_{\mu,\nu} L_\mu^*(y)\Pi_\mu\Lambda_{\mu\nu}S_\nu(y'), \tag{2}$$

suppressing the (q,ω)-dependence for the sake of brevity. The composite index $\mu[\equiv (n,n')] = \mu_\mathrm{s},\ \mu_\mathrm{a}$, with subscripts s(a) referring to the symmetric (antisymmetric) wave-function depending upon whether $n + n' =$ even (odd). This is quite a general scheme and singles out

only the symmetric structures from the asymmetric ones. The symbol $\Lambda_{\mu\nu}$ is an inverse of $(\delta_{\mu\nu} - \Pi_\mu\beta_{\mu\nu})$ such that $\sum_\nu(\delta_{\mu\nu} - \Pi_\mu\beta_{\mu\nu})\Lambda_{\nu\gamma} = \delta_{\mu\gamma}$, where $\beta_{\mu\nu} = \int dy L^*_\mu(y)S_\nu(y)$. Clearly, $L_\mu(S_\mu)$ stands for the long-range (short-range) part of the response function [20]. π_μ stands for the polarizability function. The elementary electronic excitations are determined by the poles of $\varepsilon^{-1}(y, y')$.

In Fig. 1, we summarize the wave-vector dependence of the excitation spectrum of a Q1DEG for a two subband model. Note that the sole purpose of including Fig. 1 here was to understand the correspondence between the loss-peaks predicted in this work and the excitation spectrum. Although illustrated together, the intra- and intersubband, both single-particle and collective, excitations are decoupled modes. This is because, for a symmetric potential well (as is the case here), $V_{mm'nn'}$ (the matrix elements of the Fourier transformed Coulombic interaction $V_{ee}(q, y - y') = (2e^2/\varepsilon_0)K_0(q|y - y'|)$, where $K_0(x)$ is the modified Bessel function of the second kind and ε_0 ($= 12.8$ for GaAs) is the background dielectric constant) *is strictly zero* for arbitrary momentum transfer (q) if $m + m' + n + n'$ is an odd number. It is noteworthy that the intersubband collective excitation frequency (ω^*) at $q = 0$ is almost twice the respective single-particle excitation. This shift of the intersubband resonance $\hbar\omega^*$ to energies significantly above the subband spacing ($\hbar\omega_0$) is attributed to the many-body effects, just as in 2D systems [21]. We assume that the depolarization effects are dominant and thus have $\hbar\omega^* = \hbar(\omega_0^2 + \omega_d^2)^{1/2}$, where ω_d is the depolarization frequency. In the *lack* of a desired model an upper bound on depolarization shift can be put classically [22] to yield $\omega_d^2 = 8\pi e^2 N_e^{1D}/(\tilde{\varepsilon} m^* w_{eff}^2)$. With our input parameters, this requires a constant $\tilde{\varepsilon} = 3.55\varepsilon_0$, which signals the importance of the screening effects in a quantum wire. Knowing the fact that in an experimental situation the quantization is dominant, this classical idea gives only a physical feel and is expected to grossly overestimate the depolarization effects.

Now we first discuss the rate of energy loss (W') due to a fast particle moving parallel to the Q1DEG at a distance y_0 determined through [23]

$$W' = \frac{e^2}{\pi}\mathrm{Im}\left[\int dq \int dy' \cdot (qv_x) \cdot K_0(q|y' - y_0|) \cdot \varepsilon^{-1}(q, \omega = qv_x; y_0 y')\right] \quad (3)$$

where v_x is the particle velocity along the axis of the quantum wire.

We have performed the numerical computation for the

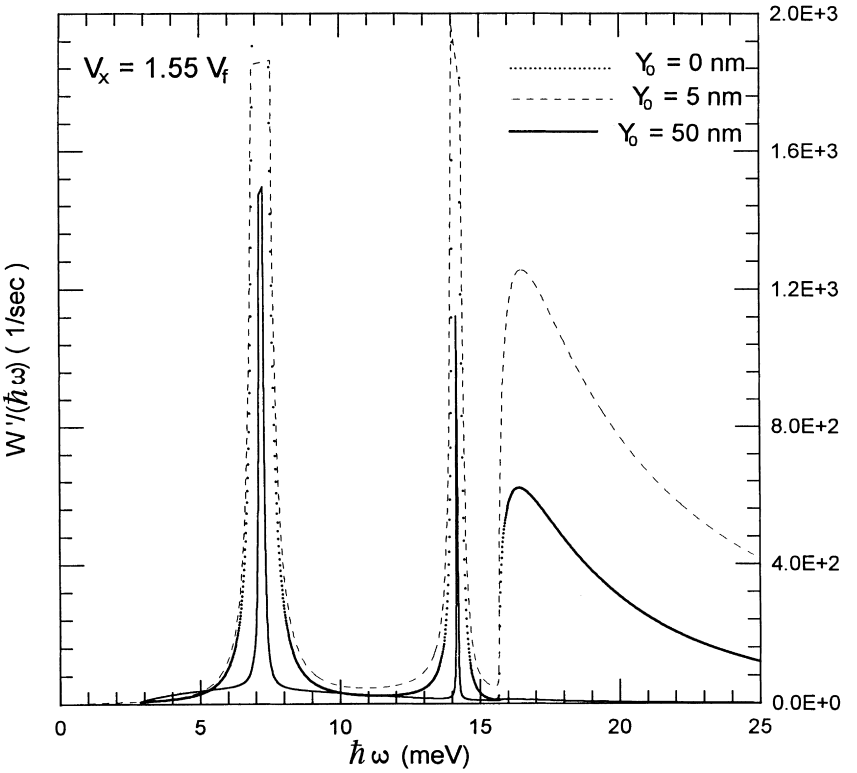

Fig. 2. The rate of energy loss per unit energy for a fast-particle moving parallel to the Q1DEG. The fast-particle velocity and its distance from the wire are as given in the figure. Note that the odd appearance of the top of the first two peaks is an artifact of constraining the *y*-axis to this value (a bad graphic software!); otherwise both of these peaks are extremely high.

rate of energy loss per unit energy. Doing so leads us to get rid of the integral over q and hence a very substantial saving in computational time is achieved, without loss of the relevant information about the loss peaks. The numerical results for a given particle velocity are illustrated for three values of y_0 in Fig. 2. One can immediately notice that the positions of the loss peaks (in energy) do not vary as a function of the distance y_0. However, it has been seen that the larger the distance between the fast-particle and Q1DEG, the smaller the rate of energy loss, just as it is expected intuitively. The first, second, and third loss peaks occurring at 7.16, 14.05, and 16.35 meV, corresponding, respectively, to $q/q_f = 0.5$, 0.98, and 1.14, explain exactly the intrasubband collective mode in the excitation spectrum (see Fig. 1). Similarly, by repeating the computation for $v_x = 2.05v_f$, we have observed three loss peaks below 25 meV—the lowest peak explains the intrasubband collective mode, whereas the two higher ones interpret the intersubband collective mode. However, for $v_x = 2.30v_f$, we observed only one broad (at 8.37 meV) and the other δ-like (at 11.62 meV) peak below 25 meV—the lower peak was seen to explain the upper edge of the intersubband single-particle excitations whereas the upper (δ-like) peak interprets the intersubband collective mode. The analogous extensive computation performed for other values of the particle velocity leads us to infer that the dominant contribution to the loss peaks comes from the collective modes (i.e. the plasmons). In this geometry, it is exclusively noteworthy that only the fast-particle velocities greater than or equal to the Fermi velocity make any sense.

Next we study the case where the fast particle is assumed to move along a prescribed path $\vec{x} \equiv \vec{x}(t) = v_x t\hat{x} + v_y t\mathrm{sgn}(t)\vec{y}$. This refers to the situation where the perpendicular component of velocity (v_y) changes the sign after (at $t = 0$) the particle impinges (at $y = -y_0$) and is specularly reflected from the surface of the Q1DEG. After rigorous algebra, we deduce the expression for probability [23]

$$P(q,\omega) = \frac{e^2\alpha}{2\pi^2\hbar\omega}\mathrm{Im}\left[\int \mathrm{d}y' \int \mathrm{d}t\cdot \mathrm{e}^{-\mathrm{i}\alpha t} \cdot F(q,\omega;v_x,v_y;y'+y_0)\cdot\varepsilon^{-1}(q,\omega;(-y_0+v_y t),y')\right] \quad (4)$$

where the Function F is defined by

$$F(q,\omega;v_x,v_y;y) = \frac{\sqrt{\pi}}{2qv_y}\int_0^\infty \mathrm{d}\xi\xi^{-3/2}\,\mathrm{e}^{-(1+c^2/q^2)/\xi} \times \mathrm{e}^{-(q^2y^2/2)\xi}\left[\mathrm{e}^{-\mathrm{i}cy}\mathrm{erfc}\left(\frac{q^2y\xi+2\mathrm{i}c}{2q\sqrt{\xi}}\right)+\mathrm{c.c.}\right] \quad (5)$$

Here $c = \alpha/v_y = (\omega - qv_x)/v_y$, and the second term in square brackets is the complex conjugate (c.c.) of the first term. The function $P(q,\omega)$ has the interpretation that $P(q,\omega)\,\mathrm{d}q\,\mathrm{d}\omega$ is the probability that the probe particle is inelastically scattered into the range of energy losses between $\hbar\omega$ and $\hbar(\omega + \mathrm{d}\omega)$ and into the range of momentum losses between $\hbar q$ and $\hbar(q + \mathrm{d}q)$. $P(q,\omega)$ completely specifies the actual kinematics of an electron at the detector.

The numerical results for a given propagation vector ($q/q_f = 0.5$) and a finite Y_0($= 10$ nm) are depicted for three values of the normal velocity (v_y) in Fig. 3. The sharp (δ-like) peaks at 7.11 and 11.14 meV explain exactly the intrasubband and intersubband collective modes in the excitation spectrum (see Fig. 1), whereas the broad peaks describe approximately the boundaries of the single-particle excitations. We repeated our computation for $q/q_f = 0.2$ and 1.0 to observe similar behavior. It should be pointed out, that, for any value of the particle-velocity, the number of loss peaks observed in the EELS is less than or equal to six, just as it is expected within a two-subband model at hand. The two δ-like peaks in the EELS spectrum occur due to the nonvanishing Dirac-delta functions associated with the imaginary parts of the polarizability functions which in turn correspond to the existence of the collective modes in the excitation spectrum. This remark is valid for all the three geometries considered in this work. It is noteworthy that the positions of the δ-like peaks (in energy) do not vary with the variation in the fast-particle velocity. This abides by the fact that the propagation vector q is kept constant for all the particle velocities. The earlier remark made with respect to plasmons as the main energy loss mechanism still remains valid.

Finally, we turn to an illustrative example of a fast particle shooting through a Q1DEG. In this case, we treat the particle velocity $\vec{v}$ = constant (fast particle shoots through) and derive the expression for probability function given by

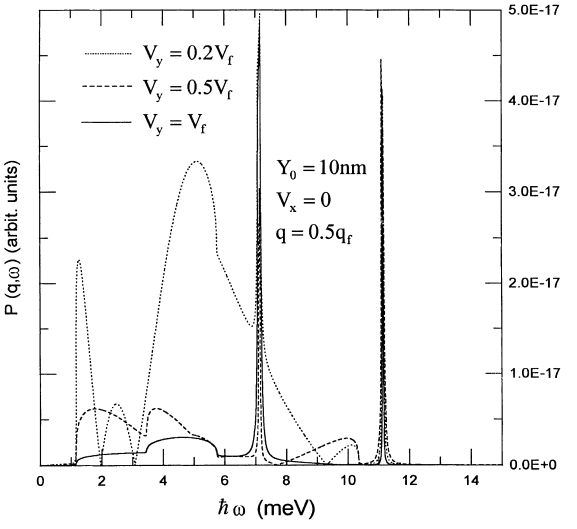

Fig. 3. The probability function $P(q,\omega)$ for a fast-particle specularly reflected from the Q1DEG. The input fast-particle velocities, the propagation vector, and the finite value of Y_0 used in the computation are given in the figure.

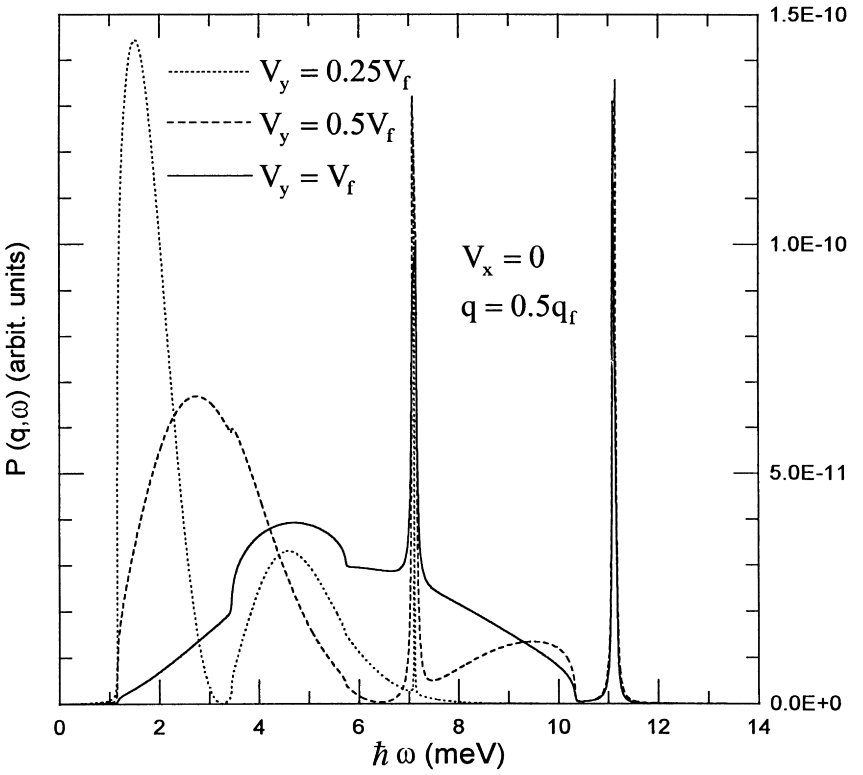

Fig. 4. The probability function $P(q, \omega)$ for a fast-particle shooting through the Q1DEG. The input fast-particle velocities and the propagation vector are given in the figure.

[23] (with $v_x \rightarrow 0$)

$$P(q,\omega) = \frac{e^2}{2\pi\hbar v_y} \frac{1}{\sqrt{\omega^2 + (qv_y)^2}}$$

$$\times \mathrm{Im}\left[\int \mathrm{d}y' \int \mathrm{d}y'' \cdot \mathrm{e}^{\mathrm{i}\omega(y'-y'')/v_y} \cdot \varepsilon^{-1}(q,\omega; y'', y') \right] \qquad (6)$$

where the symbols have their usual meanings.

The numerical results for $q/q_f = 0.5$ and for three values of the fast-particle velocity are shown in Fig. 4. Apart from some broad peaks that describe approximately the boundaries of the single-particle excitations, we observe two δ-like peaks at 7.11 and 11.12 meV that explain exactly the intrasubband and intersubband collective modes (see Fig. 1). Again, the positions of the sharp loss-peaks remain intact, eventhough the fast-particle velocity varies. Performing the computation for $q/q_f = 0.1$, 0.25, and 1.0 led us to draw similar conclusions. Just like in the other two geometries, we stress that the dominant contribution to the loss peaks comes from the intra- and intersubband collective excitations. The rest of the discussions related to previous two geometries is still valid. In spite of the fact that the main physics regarding the loss mechanism is consistent in all three geometries considered here, we feel that this geometry of fast-particle shooting through the Q1DEG yields, in general, sharper structures in the spectrum of EELS that allows sometimes better interpretation of even the single-particle excitations in the long wavelength limit. An interesting and well-defined (at long wavelengths) feature observed in this geometry is that the widths of the δ-like loss-peaks are seen to decrease with the increasing particle-velocity.

We have presented our theoretical results on the EELS in an isolated model quantum wire. The predicted loss spectra are expected to be confirmed by the so-far-unattempted HREELS (see the following paragraph), irrespective of whether such experiments are performed on an isolated quantum wire or on arrays of wires. This is because the Coulumb coupling between the neighboring wires (in the state-of-the-art high quality multiwire systems) is very weak and one is allowed to interpret the experiments performed, for sensitivity reasons, on multiwires in terms of excitations in an isolated wire.

A word on the capability of EELS for detection of these low-energy excitations in quantum wires is in order. As far as we know, no effort has so far been made to use EELS on quantum wires. The first and foremost obstacle, or so it looks like, is the thought of energy resolution of EELS concerned with the low-energy excitations in quantum wires that scares. This is true that the essential problem with this technique, which has proved to be the most

versatile and sensitive tool in surface vibration spectroscopy, has always been the resolution, which was significantly less than for the competing techniques, such as infrared spectroscopy and Raman scattering. In the latter techniques the resolution is typically about 0.25 meV, whereas in EELS a resolution of 5 meV was considered to be a good result until recently. With the increasing complexity of the problems, it became desirable to have a sensitive method with a better resolution. The technology of spectrometers is now based on *science* and excellent, easy to operate instruments capable of resolution down to 0.3 meV (theoretical limit) and 0.5 meV (experimentally achieved limit) have been built [24]. In view of this, we believe that HREELS could prove to be a potential alternative of already employed optical techniques.

We would like to draw attention to the fact that the first two geometries represent practically realizable situations. As regards the actual experiment, we believe that the (nonzero) parameter y_0 (see the text above) implicitly takes account of the expected multiple scattering and absorption of the electron beam in the host material cladding the wire. The third geometry seems to remain only of fundamental interest, unless some experimental arrangement is suggested such that the fast-particle (a coherent electron beam) can be made to shoot through the wire embedded in the host material. This is because the substrate materials lapping the Q1DEG would hardly allow the fast-particle to shoot through the whole system. However, this difficulty could possibly be surmounted in a system of quantum wires micromachined from the freely suspended 2DEG [25].

In summary, this letter predicts the first theoretical fast-particle energy loss spectra in a model quantum wire in the framework of a DRT within the full RPA. For this purpose, we made use of an exact analytical expression for the inverse dielectric function, which knows no bounds with respect to the subband occupancy. We designed the Q1DEG with a parabolic potential well to characterize the lateral confinement and worked within a two-subband model. Our main conclusion is that the dominant contribution to energy loss peaks comes from the intra- and inter-subband *collective* excitations. We hope this work will stimulate more theoretical work and encourage the experiments to evidence the capability of HREELS on the quantum wire structures. The details of the theory (incorporating explicitly the absorption in the substrate, considering larger number of occupied and unoccupied subbands, acounting for the coupling to the optical phonons, including the effects of an applied magnetic field, etc.) and numerical results are deferred to a forthcoming publication.

Acknowledgements

The authors would like to express their sincere thanks to Allan MacDonald and Aron Pinczuk for stimulating discussions and to A. Goñi and Herald Ibach for useful communications. We are grateful to Godfrey Gumbs for critical reading of the manuscript. This research was partially supported by CONACYT Grant # 28110–E.

References

[1] H. Sakaki, Jpn. J. Appl. Phys. 19 (1980) L735.
[2] H. Sakaki, Solid State Commun. 92 (1994) 119.
[3] J.M. Calleja, et al., Solid State Commun. 79 (1991) 911.
[4] A.S. Plaut, et al., Phys. Rev. Lett. 67 (1991) 1642.
[5] B.Y.K. Hu, S. Das, Sarma, Phys. Rev. Lett. 68 (1992) 1750.
[6] H.J. Schulz, Phys. Rev. Lett. 71 (1993) 1864.
[7] A.R. Goñi, et al., Phys. Rev. Lett. 70 (1993) 1151.
[8] R. Strenz, et al., Phys. Rev. Lett. 73 (1994) 3022.
[9] A. Gold, A. Ghazali, Phys. Rev. B 41 (1990) 7626.
[10] Q.P. Li, et al., Phys. Rev. B 45 (1992) 13 713.
[11] R.E. Camley, D.L. Mills, Phys. Rev. B 29 (1984) 1695.
[12] B.N.J. Persson, E. Zaremba, Phys. Rev. B 31 (1985) 1863.
[13] Ph. Lambin, J.P. Vigneron, A.A. Lucas, Phys. Rev. B 32 (1985) 8203.
[14] G. Gumbs, N.J.M. Horing, Phys. Rev. B 43 (1991) 2119.
[15] W.H. Backes, et al., Phys. Rev. B 45 (1992) 8437.
[16] T. Tsuruoka, et al., Phys. Rev. B 50 (1994) 2346.
[17] C. Lohe, et al., Phys. Rev. B 47 (1993) 3819.
[18] S.E. Laux, et al., Surf. Sci. 196 (1988) 101.
[19] S.E. Laux, F. Stern, Appl. Phys. Lett. 49 (1986) 91.
[20] M.S. Kushwaha, F. Garcia-Möliner, Phys. Lett. A 205 (1995) 217.
[21] T. Ando, A.B. Fowler, F. Stern, Rev. Mod. Phys. 54 (1982) 437.
[22] W. Hansen, et al., Application of High Magnetic Fields in Semiconductor Physics, in: G. Landwehr, et al. (Eds.), Vol. 1, Springer, Berlin, 1987, p. 266.
[23] M.S. Kushwaha, P. Zielinski, in preparation.
[24] H. Ibach, J. Electron. Spectros. Relat. Phenom. 64/65 (1993) 819.
[25] R. Blick, et al., Bull. Am. Phys. Soc. 43 (1998) 923 This work reports the first freely suspended 2DEG devices designed from AlGaAs/GaAs/AlAs heterostructures.